Chapter 3
Optical Systems with Annular Pupils

3.1 INTRODUCTION

In this chapter, we discuss the imaging properties of a system with an annular pupil in a manner similar to those for a system with a circular pupil. The two-mirror astronomical telescopes discussed in Chapter 6 of Part I are a typical example of an imaging system with an annular pupil. The linear obscuration ratios of some of the well-known telescopes are 0.36 for the 200-inch telescope at Mount Palomar, 0.37 for the 84-inch telescope at the Kitt-Peak observatory, 0.5 for the telescope at the McDonald Observatory, and 0.33 for the Hubble Space Telescope.

Expressions for the PSF, OTF, and encircled, ensquared, and excluded powers are given. The Strehl ratio of an aberrated system is considered and tolerances for primary aberrations are discussed. Symmetry properties of aberrated PSFs are discussed, and pictures of the PSFs for primary aberrations are given as examples. The line of sight of an aberrated system is discussed in terms of the centroid of its PSF. Numerical results are given and compared with the corresponding results for systems with circular pupils wherever possible and appropriate.

3.2 ABERRATION-FREE SYSTEM

We start this chapter with a discussion of the PSF, encircled, ensquared, and excluded powers, and the OTF of an aberration-free system. Equations are developed in a way that the results for a circular pupil can be obtained as a limiting case of the annular pupil. It is shown that the obscuration in an annular pupil not only blocks the light incident on it, but it also reduces the size of the central disc and increases the value of the secondary maxima of the PSF. It also increases the OTF value at high spatial frequencies while reducing it at the low frequencies.

3.2.1 Point-Spread Function

Consider, as illustrated in Figure 3-1, an aberration-free optical system imaging a point object with a uniformly illuminated annular exit pupil having outer and inner radii of a and ϵa, respectively, where ϵ is the linear obscuration ratio of the pupil. The irradiance at a point $\vec{r}_i$ in the image plane with respect to the Gaussian image point is given by Eq. (1-65), that is

$$I_i(\vec{r}_i;\epsilon) = \left[I_i\left((0;\epsilon)/S_{ex}^2(\epsilon)\right)\right]\left|\int \exp\left(-\frac{2\pi i}{\lambda R}\vec{r}_p\cdot\vec{r}_i\right)d\vec{r}_p\right|^2 , \tag{3-1}$$

where

$$S_{ex}(\epsilon) = \pi\left(1-\epsilon^2\right)a^2 \tag{3-2}$$

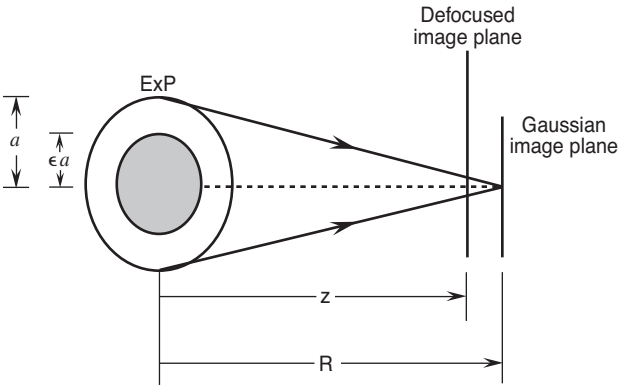

Figure 3-1. Imaging by a system with an annular exit pupil of inner and outer radii ϵa and a, respectively.

is the clear area of the obscured exit pupil. The quantity ϵ^2 in Eq. (3-2) is sometimes referred to as the area obscuration ratio. The optical wavefront at the exit pupil is spherical with a radius of curvature R and center of curvature at the Gaussian image point. The central irradiance is given by

$$I_i(0;\epsilon) = P_{ex} S_{ex}(\epsilon) / \lambda^2 R^2 \tag{3-3a}$$

$$= \pi P_{ex} \left(1 - \epsilon^2\right) / 4\lambda^2 F^2 \quad . \tag{3-3b}$$

where P_{ex} is the total power in the exit pupil, and, therefore, in the image. For an object of intensity B_o radiating at a wavelength λ at a distance z_0 from the entrance pupil of area $S_{en}(\epsilon)$, the total power is given by

$$P_{ex} = \eta \left[S_{en}(\epsilon) / z_0^2 \right] B_o \quad , \tag{3-4}$$

where η is the transmission factor of the system for light propagation from its entrance to its exit pupil. The quantity F in Eq. (3-3b) is given by

$$F = R/D \quad , \tag{3-5}$$

where $D = 2a$ is the outer diameter of the exit pupil. It represents the focal ratio (f-number) of the image-forming light cone exiting from the exit pupil. The integration in Eq. (3-1) is carried over the clear area of the exit pupil such that the position vector $\vec{r}_p$ of a point in its plane satisfies $\epsilon a \le \left| \vec{r}_p \right| \le a$.

As in Section 2.2.1, we express the position vectors of points in the pupil and image planes in polar coordinates according to

$$\vec{r}_p = r_p \left(\cos\theta_p, \sin\theta_p \right), \; \epsilon a \le r_p \le a, \; 0 \le \theta_p < 2\pi \quad , \tag{3-6}$$

and

$$\vec{r}_i = r_i\left(\cos\theta_i,\ \sin\theta_i\right),\ 0 \le \theta_i < 2\pi. \tag{3-7}$$

Substituting Eqs. (3-6) and (3-7) into Eq. (3-1), we obtain

$$I_i\left(r_i, \theta_i; \epsilon\right) = \left[I_i(0;\epsilon)/S_{ex}^2(\epsilon)\right]\left|\int_{\epsilon a}^{a}\int_{0}^{2\pi} \exp\left[-\frac{2i\pi}{\lambda R} r_p\ r_i \cos\left(\theta_p - \theta_i\right)\right] r_p\, dr_p d\theta_p\right|^2 . \tag{3-8}$$

Comparing Eqs. (2-7) and (3-8), we note that the significant difference between the two lies in the lower limit of the integration over r_p; in Eq. (2-7), the lower limit is 0, indicating an unobscured pupil; in Eq. (3-8) it is ϵ, indicating an obscured pupil. The values of S_{ex} are different in the two equations by a factor of $1-\epsilon^2$. The values of P_{ex} would also be different by this factor if the pupil irradiance were the same in both cases.

For simplicity of equations as well as numerical analysis, we use normalized quantities

$$\vec{\rho} = \vec{r}_p/a \tag{3-9a}$$

$$= \rho\left(\cos\theta_p,\ \sin\theta_p\right) , \tag{3-9b}$$

$$\vec{r} = \vec{r}_i/\lambda F \tag{3-10a}$$

$$= r\left(\cos\theta_i,\ \sin\theta_i\right) , \tag{3-10b}$$

and

$$I\left(\vec{r};\epsilon\right) = I_i\left(\vec{r}_i;\epsilon\right)\Big/\left[P_{ex}S_{ex}(0)/\lambda^2R^2\right] . \tag{3-11}$$

Note that in Eq. (3-11), we have normalized the irradiance by the central irradiance for a system with a circular pupil. Using normalized quantities, Eq. (3-8) may be written

$$I\left(r, \theta_i; \epsilon\right) = \left[\pi^2\left(1-\epsilon^2\right)\right]^{-1}\left|\int_{\epsilon}^{1}\int_{0}^{2\pi} \exp\left[-\pi i r \rho \cos\left(\theta_p - \theta_i\right)\right]\rho\, d\rho\, d\theta_p\right|^2 . \tag{3-12}$$

Integrating over θ_p by using Eq. (2-12), we obtain

$$I\left(r;\epsilon\right) = \left[4\Big/\left(1-\epsilon^2\right)\right]\left[\int_{\epsilon}^{1} J_0\left(\pi r\rho\right)\rho\, d\rho\right]^2 . \tag{3-13}$$

Carrying out the radial integration by using Eq. (2-14), we finally obtain

$$I(r;\epsilon) = \frac{1}{\left(1-\epsilon^2\right)}\left[\frac{2J_1(\pi r)}{\pi r} - \epsilon^2\,\frac{2J_1(\pi\epsilon r)}{\pi\epsilon r}\right]^2 \quad . \tag{3-14}$$

We note that the irradiance distribution is radially symmetric about the Gaussian image point $r = 0$, as may be expected for a radially symmetric (annular) pupil function. It is *not* normalized to unity at the center. Its central value is given by $1-\epsilon^2$. Except for a normalization factor, Eq. (3-14) also gives the PSF of the system. It follows from Eq. (1-61) that

$$PSF(\vec{r}_i;\epsilon) = I_i(\vec{r}_i;\epsilon)\big/P_{ex} \tag{3-15}$$

We note that as $\epsilon \to 0$, Eq. (3-14) for the annular pupil reduces to Eq. (2-15) for the circular pupil. In order that the total power be the same for the two pupils, the irradiance across the annular pupil must be higher than that for a circular pupil by a factor of $\left(1-\epsilon^2\right)^{-1}$. For a given total power P_{ex} in the exit pupil, the central irradiance $I(0;\epsilon)$ is smaller by a factor of $1-\epsilon^2$ compared to that for a circular pupil. However, if the pupil irradiance is the same in both cases, as in astronomical observations, then $P_{ex}(\epsilon)$ is also smaller than $P_{ex}(0)$ by a factor of $1-\epsilon^2$. Hence, $I(0;\epsilon)$ will be smaller than $I(0;0)$ by a factor of $\left(1-\epsilon^2\right)^2$.

The principal maximum of the image irradiance distribution lies at the Gaussian image point $r = 0$, since all the Huygens' spherical wavelets originating at the spherical wavefront in the exit pupil arrive in phase at this point and, accordingly, interfere constructively. From Eq. (3-14), we note that the image irradiance is zero at those values of *r* for which

$$J_1(\pi r) = \epsilon J_1(\pi\epsilon r),\ r \neq 0 \quad . \tag{3-16}$$

These values of *r* locate the *minima* of the irradiance distribution. Noting Eq. (2-19), we find that the *secondary maxima* lie at those values of *r* that satisfy

$$J_2(\pi r) = \epsilon^2 J_2(\pi\epsilon r),\ r \neq 0 \quad . \tag{3-17}$$

The irradiance distribution for a system with a very thin annulus pupil $(\epsilon \to 1)$ may be obtained from Eq. (3-13) by noting that $\rho \simeq 1$, and the variation of $J_0(\pi r\rho)$ is negligibly small over the variation of ρ that it can be replaced by $J_0(\pi r)$. Hence, Eq. (3-13) reduces to

$$I(r;\epsilon \to 1) = J_0^2(\pi r) \tag{3-18}$$

when normalized by the central irradiance $P_{ex}S_{ex}(\epsilon)\big/\lambda^2 R^2$.

3.2.2 Encircled Power

The amount of power in the image plane contained in a circle of radius r_c centered at the Gaussian image point is given by

$$P_i(r_c;\epsilon) = 2\pi \int_0^{r_c} I_i(r_i;\epsilon)\, r_i\, dr_i \quad . \tag{3-19}$$

Substituting Eqs. (3-10a) and (3-11) into Eq. (3-19) and defining a normalized or fractional *encircled power*

$$P(r_c;\epsilon) = P_i(r_c;\epsilon)/P_{ex} \quad , \tag{3-20}$$

we obtain

$$P(r_c;\epsilon) = \left(\pi^2/2\right) \int_0^{r_c/\lambda F} I(r;\epsilon)\, r dr \quad . \tag{3-21}$$

If we let r_c be in units of λF and substitute Eq. (3-14) into Eq. (3-21), we obtain

$$P(r_c;\epsilon) = \frac{1}{1-\epsilon^2}\left[P(r_c) + \epsilon^2 P(\epsilon r_c) - 4\epsilon \int_0^1 J_1(\pi r_c u)\, J_1(\pi\epsilon r_c u)\, \frac{du}{u} \right] \quad , \tag{3-22}$$

where

$$P(r_c) = 1 - J_0^2(\pi r_c) - J_1^2(\pi r_c) \tag{3-23}$$

is the encircled power for a system with a circular exit pupil.

3.2.3 Ensquared Power

The *ensquared power* in a square region of half-width r_s centered on the Gaussian image point in the image plane is given by[1]

$$P_i(r_s;\epsilon) = \iint_{r_s} I_i(r_i;\epsilon)\, r_i\, dr_i\, d\theta_i \quad , \tag{3-24}$$

where the integration is carried over the square region. Following the same procedure as in the case of circular pupils (see Section 2.2.3), Eq. (3-24) reduces to

$$P_s(r_s;\epsilon) = P_c\left(\sqrt{2} r_s;\epsilon\right) - \frac{8}{\pi\left(1-\epsilon^2\right)} \int_1^{\sqrt{2}} \left[J_1(\pi r_s u) - \epsilon J_1(\pi\epsilon r_s u)\right]^2 \cos^{-1}(1\ u)\, \frac{du}{u} \quad , \tag{3-25}$$

where

$$P_s(r_s;\epsilon) = P_i(r_s)/P_{ex} \tag{3-26}$$

and

$$P_c(r_c) = P(r_c) \tag{3-27}$$

are the fractional ensquared and encircled powers, respectively, and r_s and r_c are in units of λF. The first term on the right-hand side of Eq. (3-25) represents the image power contained in a circle of radius $\sqrt{2}r_s$. The second term gives the image power contained in a region lying between a circle of radius $\sqrt{2}r_s$ and a square of full-width $\sqrt{2}r_s$. Both of these terms require numerical integration.

3.2.4 Excluded Power

The *excluded image power* X_i, i.e., the power contained outside a certain area in the image plane can be calculated quite accurately in closed form if the included area is large enough so that $X_i \le 0.1\, P_{ex}$. For large arguments we can use the asymptotic expression for Bessel functions; namely, Eq. (2-33). Thus, for large values of *r*, Eq. (3-14) can be written

$$I(r;\epsilon) = \frac{8}{\pi^4 r^3\left(1-\epsilon^2\right)}\left[\sin\pi\left(r-1/4\right)-\sqrt{\epsilon}\,\sin\pi\left(\epsilon r-1/4\right)\right]^2 \quad . \tag{3-28}$$

Noting that the average of a sine square is half and the average of the product of two sines with different arguments is zero, the average irradiance (indicated by a bar) for large values of *r* may be written

$$\bar{I}(r;\epsilon) \simeq \frac{4}{\pi^4 r^3(1-\epsilon)} \quad . \tag{3-29}$$

Hence, the excluded encircled power is given by

$$X_c(r_c;\epsilon) \simeq \left(\pi^2/2\right)\int_{r_c}^{\infty} \bar{I}(r;\epsilon)\, r\, dr$$

$$= \frac{2}{\pi^2 r_c(1-\epsilon)} \quad , \tag{3-30}$$

and the excluded ensquared power is given by

$$X_s(r_s;\epsilon) \simeq \int_{|x|>r_s} dx \int_{|y|>r_s} dy \bar{I}(r;\epsilon)$$

$$= \frac{4\sqrt{2}}{\pi^3 r_s(1-\epsilon)} \quad , \tag{3-31}$$

where $r = \left(x^2 + y^2\right)^{1/2}$ and the subscripts *c* and *s* on *X* indicate a large circular or a square region of exclusion centered on the Gaussian image point. From Eqs. (3-30) and (3-31), we note that

$$X_s(r_c;\epsilon) = 0.9\, X_c(r_c;\epsilon) \quad . \tag{3-32}$$

The factor of 0.9 between X_s and X_c is independent of ϵ. We also note that excluded power for an annular pupil is larger by a factor of $(1-\epsilon)^{-1}$ compared to that for a corresponding circular pupil.

The approximate result of Eq. (3-29) and those that follow from it, although obtained for the aberration-free case, are valid even when aberrations are present in the system. This may be seen by substituting Eq. (3-42) given later into Eq. (1-154) and considering the normalizations used in Eq. (3-29). It should be noted, however, that the value of *r* for which Eq. (3-29) is valid increases as aberrations are introduced into the system.

3.2.5 Numerical Results

Figure 3-2 shows the irradiance distribution and encircled power for several values of ϵ including zero. The irradiance is normalized to unity at the center in Figure 3-2b. The values of *r* for the first several minima are given in Table 3-1 for $\epsilon = 0(0.1)0.9$. We note that the radius of the central bright disc (first dark ring) decreases monotonically as ϵ increases. As $\epsilon \to 1$, this radius approaches a value of 0.76 [first zero of $J_0(\pi r)$] compared to a value of 1.22 [first zero of $J_1(\pi r)$] when $\epsilon = 0$. Moreover, the secondary maxima become higher as ϵ increases. For example, when $\epsilon = 0.5$, the first secondary maximum has a value of 9.63% of the principal maximum compared to a value of 1.75% for a circular pupil. The radius of the second dark ring first increases with ϵ, achieves its maximum value for $\epsilon = 0.4$, and then decreases. The radius of the third dark ring first decreases, then increases, achieving its maximum value for $\epsilon = 0.5$, and then decreases again. The radius of the fourth dark ring first increases, then decreases, increases again, and finally decreases as ϵ increases.

Figure 3-3 shows the irradiance distribution given by Eq. (3-14) for $\epsilon = 0$, 0.25, 0.5, and 0.75 normalized to unity at the center. This figure and Table 3-2 also show how P_c, P_s and $P_s - P_c$ vary with r_c in graphical and tabulated forms. The value of P_c in a given dark ring decreases or increases with ϵ in a manner similar to how its radius varies, although a peak or a valley in its variation is not achieved for the same value of ϵ. For small values of ϵ, the first maximum of $P_s - P_c$ is the highest. However, for large values of ϵ one of the secondary maxima is the highest. As ϵ increases, the secondary maxima of irradiance become increasingly more significant, and therefore, Eqs. (3-30) and (3-31) give accurate results for increasingly larger values of r_c and r_s, respectively. For example, if the difference between actual results (given in Table 3-2) and those obtained from Figure 3-2 is to be less than 2.6% of the total power, r_c must be larger than 1.7, 1.8, and 3.8 when ϵ is equal to 0.25, 0.50, and 0.75, respectively. A general rule of thumb is